

# Emergent hyperuniformity in periodically-driven emulsions

Joost H. Weijs,<sup>1</sup> Raphaël Jeanneret,<sup>2</sup> Rémi Dreyfus,<sup>3</sup> and Denis Bartolo<sup>1</sup>

<sup>1</sup>*Laboratoire de Physique de l'École Normale Supérieure de Lyon,  
Université de Lyon, 46, allée d'Italie, 69007 Lyon, France*

<sup>2</sup>*Department of Physics, University of Warwick, Coventry, CV4 7AL, United Kingdom*

<sup>3</sup>*Complex Assemblies of Soft Matter, CNRS-Solvay-UPenn UMI 3254, Bristol, Pennsylvania 19007-3624, USA*

(Dated: September 4, 2018)

We report the emergence of large-scale hyperuniformity in microfluidic emulsions. Upon periodic driving confined emulsions undergo a first-order transition from a reversible to an irreversible dynamics. We evidence that this dynamical transition is accompanied by structural changes at all scales yielding macroscopic yet finite hyperuniform structures. Numerical simulations are performed to single out the very ingredients responsible for the suppression of density fluctuations. We show that as opposed to equilibrium systems the long-range nature of the hydrodynamic interactions are not required for the formation of hyperuniform patterns, thereby suggesting a robust relation between reversibility and hyperuniformity which should hold in a broad class of periodically driven materials.

PACS numbers: 05.65.+b, 47.57.Bc, 05.70.Ln

What is the most effective way to homogeneously fill space with an ensemble of particles? At thermal equilibrium, an obvious effective strategy would be to endow the particles with interactions promoting the formation of a crystal. In a  $d$ -dimensional system, thermal fluctuations would spontaneously organize the particles into an ordered state where the fluctuations of the number of particles enclosed in a box of size  $\ell$  would scale as  $\Delta N_\ell^2 \sim \ell^{d-1}$ : crystals are hyperuniform [1]. At large scales, they are much more homogeneous than a random set of points with number fluctuations of the order of the box volume  $\ell^d$ . However crystals are not the only patterns being hyperuniform [1, 2]. Over the last decade much attention has been devoted to disordered structures displaying miniature density fluctuations. As it turns out such hyperuniform patterns have been shown to display outstanding optical properties such as complete photonics band gaps [3–5]. Until very recently the only two controlled strategies to engineer hyperuniform materials were based on numerical optimization techniques [3, 5, 6], or the jamming of athermal hard spheres [7–11]. In 2015, two sets of numerical simulations have demonstrated that hyperuniformity emerges when ensembles of particles driven out of equilibrium approach a critical absorbing phase transition [12, 13]. However, these numerical models based on elegant toy models lack a truly analogous physical system, in which hyperuniformity emerges from genuine physical interactions.

In this letter we demonstrate experimentally that, when periodically driven, microfluidic emulsions self-organize into macroscopic (yet finite) hyperuniform structures. We evidence that maximal hyperuniformity is reached at the onset of reversibility of the droplet dynamics, even though the emulsion does not display any critical feature and does not reach a genuine absorbing state either. We also identify the minimal ingredients required to produce hyperuniform emulsions by means

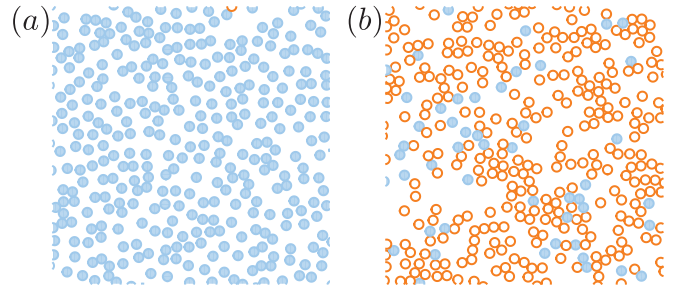


FIG. 1: Close-up of the emulsion at the beginning of the 500th cycle. The active droplets are shown as open orange circles, the passive droplets as filled blue circles. (a) For a driving amplitude  $\Delta/\Delta^* = 0.65$ , the dynamics is reversible. (b) For a driving amplitude  $\Delta/\Delta^* = 1.54$ , the dynamics is not reversible anymore. Note also the markedly different structure in the two cases: for low amplitudes the structure is more homogeneous.

of numerical simulations. Surprisingly, unlike in equilibrium systems, we show that long-range interactions are not necessary to yield extended hyperuniform structures. We therefore conjecture that hyperuniformity is intimately related to reversibility in periodically driven systems, and should therefore be achieved in a broad class of hard and soft condensed matter materials.

The experimental setup is the one used in [14] consisting of flowing a monodisperse emulsion (area fraction:  $0.36$ ) in a microfluidic channel ( $0.5 \text{ cm} \times 5 \text{ cm} \times 27 \pm 0.1 \mu\text{m}$ ). The droplets have a diameter  $a = 25.5 \pm 0.5 \mu\text{m}$  comparable to the height of the channel and therefore undergo two-dimensional motion. The inlet of the channel is connected to a syringe pump that drives the suspension sinusoidally. The emulsion is prepared in a reproducible initial state reached after a sequence of 10 high-amplitude oscillations. Then, a sequence of  $10^3$  cycles at the desired

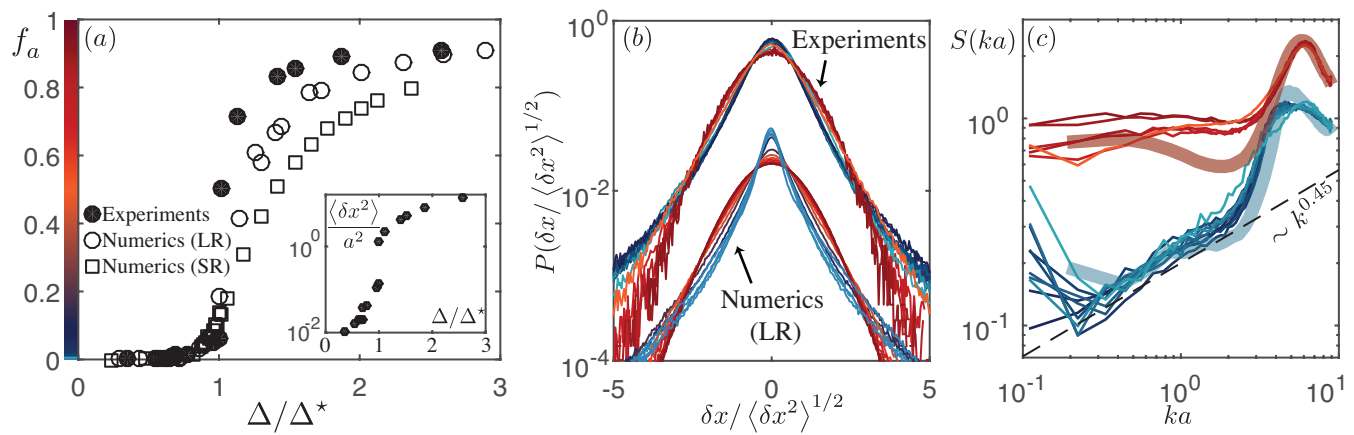


FIG. 2: (a) Fraction of active particles  $f_a$  in the steady state at various oscillation amplitudes. At  $\Delta = \Delta^*$  reversibility abruptly breaks down. Inset: Variations of the mean-squared strobed displacement in the flow direction  $\langle \delta x^2 \rangle$  plotted as a function of  $\Delta$ . (b) Centered and normalized probability density distribution of the strobed displacements of the droplets,  $\delta x$ , in the flow direction for the experiments (top curves) and numerics (bottom curves). The numerical curves have been shifted for sake of clarity. The color indicates the mean fraction of active particles. See colorbar in (a). (c) Structure factor  $S(k)$  at various amplitudes (Experiments: thin lines, simulations: Thick lines, Same color code as in (b)). For sake of clarity the curves corresponding to  $\Delta < \Delta^*$  have been shifted down by a constant value. The dashed line is a guide and corresponds to  $k^{0.45}$ .

amplitude is applied to ensure that the measurements are performed in a statistically stationary state. The mean displacement of the droplets occurs along the main flow direction and is sinusoidal, and its amplitude  $\Delta$  is the sole control parameter of the experiments. Data is collected by tracking the instantaneous position of  $\sim 3 \times 10^3$  droplets remaining in the field of view throughout the entire flow cycle. Two snapshots of the emulsion are shown in Fig. 1 and correspond to  $\Delta = 18.3a$  and  $\Delta = 43.3a$  respectively.

Following [15] the macroscopic reversibility of the system is measured by determining the fraction of active particles  $f_a$ , which is the fraction of droplets that behave irreversibly. A droplet is here defined to be *active* if it does not return at the end of a cycle within the spatial extent of the Voronoï cell it occupied at the start of the cycle. In these experiments  $Re \ll 1$ , the fluid flows are therefore reversible in time [14]. However, above a driving amplitude  $\Delta^*/a = 28.1 \pm 0.3$  the droplet dynamics abruptly becomes irreversible. A macroscopic fraction of the droplets remains endlessly active upon periodic driving as illustrated in Fig. 1, and quantified in Fig. 2a where  $f_a$  is plotted as a function of driving amplitude.

As the order parameter  $f_a$  is based on a metric-free criteria, it is both affected by the changes in the dynamics, and in the structure of the emulsion. We now disentangle and elucidate these two concomitant collective phenomena. Let us begin with the dynamical arrest of the strobed dynamics. The reversible states where droplets retrace their steps back to their initial Voronoï cell,  $\Delta < \Delta^*$ , do not correspond to interaction-free conformations: the passive droplets continuously interact with their neighbors via hydrodynamic interactions in

the course of the cycles. They also a priori experience a number of weak but irreversible perturbations such as short-range potential interactions, or minute shape deformations which cannot be experimentally measured. As a result, even in the reversible regime, they return only *on average* to their initial position after a cycle. The transition to an irreversible regime where all the particles are active is associated to a discontinuous amplification of the mean-square displacement of the strobed dynamics, thereby causing the escape of the droplets from their initial Voronoï cell, see Figure 2a inset. We characterize the fluctuations of the strobed dynamics by the distribution of the displacements at the end of each cycle in Figure 2b. At the onset of irreversibility this distribution is not merely widened, the statistics of the droplet displacements becomes qualitatively different at  $\Delta^*$  thereby confirming the discontinuous nature of the dynamical transition. Surprisingly, whereas the strobed-displacement statistics is Gaussian for high  $\Delta$ , it is exponential in the reversible regime, echoing the existence of rare large-amplitude jumps when the droplets exit their Voronoï cell. These intermittent displacements are akin to the cage jumps found in glass forming liquids [16]. Importantly, these results imply that the dynamical arrest of the strobed dynamics does not belong to the absorbing-phase-transition scenario reported in [12, 13, 15, 17].

We now focus on the central results of this letter and demonstrate the emergence of hyperuniformity. Having a quick look back at Fig. 1, we see that the configuration in the reversible regime looks much more homogeneous than in the irreversible regime. In order to quantify this apparent structural change, we compute the structure factor  $S(k)$  of the emulsion at various amplitudes, Fig. 2c.

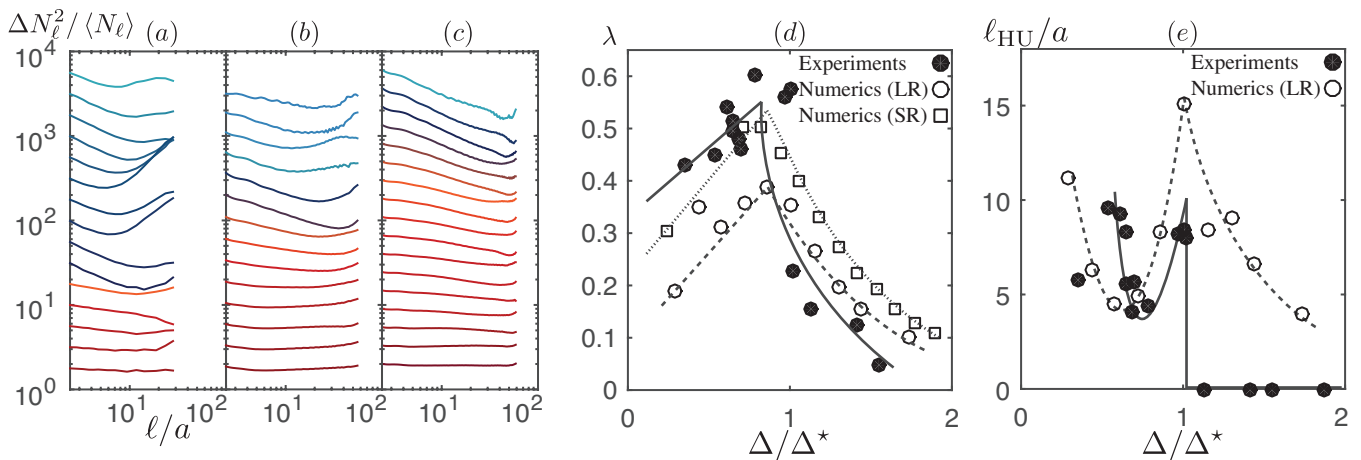


FIG. 3: (a), (b) and (c) Normalized density fluctuations for experiments (a), simulations with long-range interactions (b), and short-range interactions (c). At high amplitudes (red curves) the density fluctuations are normal, whereas in the reversible regime, at low amplitudes (blue curves), the density fluctuations are suppressed. (d) Fitted power-law exponents  $\lambda$  from the curves plotted in (a), (b) and (c). The lines are guides to the eye. Density fluctuations are only suppressed for  $\Delta \lesssim \Delta^*$ . (e) Extent of the hyperuniform regions  $\ell_{HU}$ . Filled symbols: experiments, open symbols: simulations. The lines are guides to the eye. The system is only hyperuniform up to length-scales of  $\sim 10a$  (resp.  $\sim 15a$ ) in the experiments (resp. in the simulations).

The existence of a structural transition at the onset of reversibility is very noticeable from the sudden change of  $S(k)$  across all scales. The shift of the high- $k$  peak of the structure factor corresponds to the change of the liquid-like structure reported in [14]. However the most striking feature at the transition occurs at low  $k$ . For high driving amplitudes (upper curves),  $S(k)$  plateaus to a finite value as  $k$  goes to 0, indicating the absence of long-range order. In contrast, at low amplitudes (lower curves)  $S(k)$  decays algebraically as  $k$  goes to 0, large-scale density fluctuations are suppressed [1]. The emulsion self-organizes into a hyperuniform state.

In order to quantify the degree of hyperuniformity and the extent of the hyperuniform regions, we go back to real space and directly measure the statistics of the droplet number  $N_\ell$  in a  $\ell \times \ell$  box [1, 12]. Figure 3a shows the variations of the variance  $\Delta N_\ell^2 \equiv \langle N_\ell^2 \rangle - \langle N_\ell \rangle^2$  normalized by  $\langle N_\ell \rangle$  as a function of  $\ell$ . Any ensemble of particles with no spatial correlation whatsoever has a variance that scales as  $\Delta N_\ell^2 \sim \langle N_\ell \rangle$ . Therefore,  $\Delta N_\ell^2 / \langle N_\ell \rangle$  is a decreasing function of  $\ell$  for hyperuniform systems. In Figure 3a we quantify the level of hyperuniformity of the emulsions by normalizing the variance  $\Delta N_\ell^2$  by that of a random set of points of the same size and density. This procedure is used to minimize any statistical artifacts due to the finite sample size. For sake of clarity we have shifted the curves starting from small driving amplitudes at the top. For large drivings ( $\Delta \gg \Delta^*$ ),  $\Delta N_\ell^2 / \langle N_\ell \rangle$  does not show any significant variations. The density fluctuations are normal. Conversely, as the dynamics becomes reversible ( $\Delta < \Delta^*$ ), the emulsion becomes locally hyperuniform.  $\Delta N_\ell^2 / \langle N_\ell \rangle$  indeed first decays algebraically with  $\ell$  up to

a box size  $\ell_{HU}$  above which it increases. We expect the variations to then saturate for high values of  $\ell$  that are not accessible with our experimental setup. This non-monotonic behavior is very similar to the one reported first in [12], at the onset of an absorbing phase transition.

More quantitatively, the system homogeneity is quantified by the exponent  $\lambda > 0$  defined as:  $\Delta N_\ell^2 / \langle N_\ell \rangle \propto \ell^{-\lambda}$ . For a random set of points  $\lambda = 0$ , while  $\lambda = 1$  for perfect crystals. In Fig. 3(b) the exponent  $\lambda$  fitted for small  $\ell$  is shown as a function of the driving amplitude  $\Delta$ . Interestingly, the closer the system to the reversibility transition, the more the density fluctuations are suppressed. At  $\Delta = \Delta^*$ , we find that  $\lambda \sim 0.5$  which is again close to the one reported for systems close to an absorbing phase transition ( $\lambda \sim 0.45$ ) in [12] and in [13] at intermediate scales.

The extent of the hyperuniform regions is characterized by measuring the length  $\ell_{HU}$  where  $\Delta N_\ell^2 / \langle N_\ell \rangle$  deviates from a decreasing power law, Fig. 3(c) [18]. This length-scale undergoes non-monotonic variations with the driving amplitude. When increasing  $\Delta$ ,  $\ell_{HU}$  decays from ten to five droplet diameters around  $\Delta/\Delta^* \sim 0.7$ . Then approaching the reversibility transition  $\ell_{HU}$  increases again to its maximal value ( $\sim 10a$ ) before dropping down to zero above  $\Delta^*$ . Two comments are in order. Firstly, we do not see any sign of a divergence of  $\ell_{HU}$  as  $\Delta$  approaches  $\Delta^*$ , which means that the emulsion never self-organizes into a fully hyperuniform state where the density fluctuations would be suppressed at the entire system scale. However, the typical extent of the hyperuniform regions are much larger than the typical distance below which the droplets display translational order. The pair correlation function of the emulsion decays exponentially

over distances that are at most of the order of a couple of particle diameters [18]. Secondly, the rather complex variations of  $\ell_{HU}$  contrasts with that of all the other structural, and dynamical quantities which only display a significant change at the transition point  $\Delta^*$ . A potential explanation is that the intrinsic slowing down of the strobed dynamics below  $\Delta^*$  makes the hyperuniform self-organization too slow to be experimentally achieved, although all the other (local) observables have reached a steady state.

What causes this emulsion to self-organize into hyperuniform large-scale structures? The droplets in the experimental system interact through various forces: hydrodynamic forces that are time reversible, but also short-range irreversible forces such as depletion, van der Waals, and electrostatic forces which are specific to the nature of the fluids and surfactants forming the emulsion. To find out which of these ingredients are relevant to achieve hyperuniformity, we perform numerical simulations using a model containing only minimal hydrodynamic interactions and steric repulsion due to the finite size of the droplets. The flow induced by a moving droplet in a geometry as used in the experiment is described by a potential-flow dipole [19]. Each of the 896 droplets is advected by the local flow  $\mathbf{u}(\mathbf{r})$  with the friction being modeled through a mobility coefficient  $0 < \mu < 1$ . The equation of motion for droplet  $i$  is  $\dot{\mathbf{r}}_i = \mu \mathbf{u}(\mathbf{r}_i)$ . Assuming pairwise additive interactions, the flow at the location of particle  $i$  is  $\mathbf{u}(\mathbf{r}_i)$  is the sum of the contributions from the driving flow  $\mathbf{u}_0$ , and from the flow induced  $\mathbf{u}_j$  by all other particles  $i \neq j$  in the system. The full equations of motion are:

$$\dot{\mathbf{r}}_i = \mu \left( \mathbf{u}_0(t) + \sum_{j \neq i} \frac{2\hat{\mathbf{r}}_{ij}\hat{\mathbf{r}}_{ij} - \mathbb{1}}{2\pi|\mathbf{r}_{ij}|^2} \cdot \boldsymbol{\sigma}_j \right), \quad (1)$$

where  $\boldsymbol{\sigma}_j$  is the dipole-vector associated with the particle  $j$ . The strength of the dipole is proportional to the velocity of this particle relative to the ambient fluid. The boundary conditions in the flow-direction are periodic, whereas the flow is bounded by walls in the transverse direction. The infinite number of dipole-images that arise due to this are modeled analogous as in [20] and is described in the supplementary materials [18].

This minimal model correctly accounts both for the dynamical and structural transitions. A reversible-to-irreversible transition occurs as the driving amplitude  $\Delta$  is varied, Fig. 2a, open symbols. The dipole strength which is our sole free parameter, is set to match the experimental value of  $\Delta^*$ . Without any additional adjustment, we see that the same dynamical changes occur as in the experiments, Fig. 2b. The shape of the probability density abruptly changes from a Gaussian to an exponential across the reversibility transition as observed in the experiments. Similarly, the structure above and below the transition are markedly different at all scales,

Fig. 2c. Again the computed structure factor share the same salient features as the experimental one. Importantly, our simulations quantitatively captures the emergent hyperuniform structures in the reversible regime, Fig. 3. Both the exponent  $\lambda$  and the extent  $\ell_{HU}$  of the hyperuniform regions are consistent with the experimental measurements, Fig. 3b,c. This agreement unambiguously demonstrates (i) that hyperuniformity chiefly stems from the combination of reversible hydrodynamic interactions and short-range repulsion, and (ii) that this phenomenology is robust to the very details of the interactions between the droplets and of their near-field flows.

In order to gain more physical insight, we now question the importance of the long-range ( $\sim r^{-2}$  in 2D) nature of the interactions, which are very specific to hydrodynamics. Long-ranged interactions can yield hyperuniformity in systems at thermal equilibrium such as one-component plasmas [21]. A natural question is therefore: does the emergence of hyperuniformity depend on the long-range nature of the particle-particle interactions in this non-equilibrium system as well? To answer this question, we perform the same simulations as above, but apply a very short-ranged exponential screening to the hydrodynamic interactions of the form  $\exp(-|\mathbf{r}_{ij}|/a)$ , keeping all the other parameters unchanged. Choosing a screening length of one particle diameter prevents the droplets from interacting over the observed hyperuniformity length scale while preserving the reversible nature of the microscopic dynamics. As is evident from Fig. 2a, the same reversible-to-irreversible transition, yet smoother, is observed thereby further demonstrating the robustness of our main findings. Counterintuitively, the extent of the hyperuniform regions is clearly not reduced by screening, conversely it is extended up to the entire simulation window. As opposed to equilibrium systems, long-ranged interactions impair hyperuniform self-organization. This counterintuitive observation might be explained by a critical reversibility transition when the interactions are short-range, as suggested by the sharp increase of the structural relaxation time at  $\Delta^*$  [18]. This picture is consistent with the results reported in [15] where hydrodynamic interactions are short-ranged and the transition critical. However, a thorough finite-size scaling analysis would be required to unambiguously confirm that long-range interactions suppress criticality in our system.

Together with that of [12, 13], our experimental and numerical results strongly suggest that any ensemble of particles at the onset of a reversible-to-irreversible transition self-organizes into hyperuniform patterns. A broad class of materials are therefore expected to self-assemble into hyperuniform structures upon periodic driving, from colloidal suspensions [15, 22–24], to soft glasses [25], to shaken grains [26] to vortices in superconductors [27].

We thank L. Berthier, P. Chaikin and S. Torquato for insightful discussions. We acknowledge support support from Institut Universitaire de France (D. B.), and the

NWO-Rubicon programme financed by the Netherlands Organisation for Scientific Research (JHW).

- 
- [1] S. Torquato and F. H. Stillinger, *Local density fluctuations, hyperuniformity, and order metrics*, Phys. Rev. E **68**, 041113 (2003).
- [2] C. E. Zachary and S. Torquato, *Hyperuniformity in point patterns and two-phase random heterogeneous media*, Journal of Statistical Mechanics: Theory and Experiment **2009**, P12015 (2009).
- [3] M. Florescu, S. Torquato, and P. J. Steinhardt, *Designer disordered materials with large, complete photonic band gaps*, Proc. Nat. Acad. Sci. USA **106**, 20658 (2009).
- [4] W. Man, M. Florescu, K. Matsuyama, P. Yadak, G. Nahal, S. Hashemizad, E. Williamson, P. Steinhardt, S. Torquato, and P. Chaikin, *Photonic band gap in isotropic hyperuniform disordered solids with low dielectric contrast*, Opt. Express **21**, 19972 (2013).
- [5] W. Man, M. Florescu, E. P. Williamson, Y. He, S. R. Hashemizad, B. Y. C. Leung, D. R. Liner, S. Torquato, P. M. Chaikin, and P. J. Steinhardt, *Isotropic band gaps and freeform waveguides observed in hyperuniform disordered photonic solids*, Proc. Nat. Acad. Sci. USA **110**, 15886 (2013).
- [6] R. D. Batten, F. H. Stillinger, and S. Torquato, *Classical disordered ground states: Super-ideal gases and stealth and equi-luminous materials*, Journal of Applied Physics **104**, 033504 (2008).
- [7] A. Donev, F. H. Stillinger, and S. Torquato, *Unexpected Density Fluctuations in Jammed Disordered Sphere Packings*, Phys. Rev. Lett. **95**, 090604 (2005).
- [8] C. E. Zachary, Y. Jiao, and S. Torquato, *Hyperuniform Long-Range Correlations are a Signature of Disordered Jammed Hard-Particle Packings*, Phys. Rev. Lett. **106**, 178001 (2011).
- [9] L. Berthier, P. Chaudhuri, C. Coulais, O. Dauchot, and P. Sollich, *Suppressed Compressibility at Large Scale in Jammed Packings of Size-Disperse Spheres*, Phys. Rev. Lett. **106**, 120601 (2011).
- [10] R. Kurita and E. R. Weeks, *Experimental study of random-close-packed colloidal particles*, Phys. Rev. E **82**, 011403 (2010).
- [11] R. Dreyfus, Y. Xu, T. Still, L. A. Hough, A. G. Yodh, and S. Torquato, *Diagnosing hyperuniformity in two-dimensional, disordered, jammed packings of soft spheres*, Phys. Rev. E **91**, 012302 (2015).
- [12] D. Hexner and D. Levine, *Hyperuniformity of Critical Absorbing States*, Phys. Rev. Lett. **114**, 110602 (2015).
- [13] E. Tjhung and L. Berthier, *Hyperuniform Density Fluctuations and Diverging Dynamic Correlations in Periodically Driven Colloidal Suspensions*, Phys. Rev. Lett. **114**, 148301 (2015).
- [14] R. Jeanneret and D. Bartolo, *Geometrically protected reversibility in hydrodynamic Loschmidt-echo experiments*, Nat. Comm. **5**, (2014).
- [15] L. Corte, P. M. Chaikin, J. P. Gollub, and D. J. Pine, *Random organization in periodically driven systems*, Nat. Phys. **4**, 420 (2008).
- [16] P. Chaudhuri, L. Berthier and W. Kob *Universal Nature of Particle Displacements close to Glass and Jamming Transitions* Phys. Rev. Lett. **99**, 060604 (2007)
- [17] G. I. Menon and S. Ramaswamy, *Universality class of the reversible-irreversible transition in sheared suspensions*, Phys. Rev. E **79**, 061108 (2009).
- [18] We carefully describe in a supplementary document: (i) how  $\ell_{\text{HU}}$  is measured, (ii) the numerical method, (iii) the decay of the pair-correlation function and (iv) the increase of the structural relaxation time.
- [19] T. Beatus, T. Tlusty, and R. Bar-Ziv, *Phonons in a one-dimensional microfluidic crystal*, Nature Physics **2**, 743 (2006).
- [20] A. Lefauve and D. Saintillan, *Globally aligned states and hydrodynamic traffic jams in confined suspensions of active asymmetric particles*, Phys. Rev. E **89**, 021002 (2014).
- [21] D. Levesque, J. J. Weis, and J. L. Lebowitz, *Charge fluctuations in the two-dimensional one-component plasma*, Journal Of Statistical Physics **100**, 209 (2000).
- [22] D. Pine, J. Gollub, J. Brady, and A. Leshansky, *Chaos and threshold for irreversibility in sheared suspensions*, Nature **438**, 997 (2005).
- [23] J. D. Paulsen, N. C. Keim, and S. R. Nagel, *Multiple Transient Memories in Experiments on Sheared Non-Brownian Suspensions*, Phys. Rev. Lett. **113**, 068301 (2014).
- [24] N. C. Keim and P. E. Arratia, *Mechanical and Microscopic Properties of the Reversible Plastic Regime in a 2D Jammed Material*, Phys. Rev. Lett. **112**, 028302 (2014).
- [25] K. Hima Nagamanasa, S. Gokhale, A. K. Sood, and R. Ganapathy, *Experimental signatures of a nonequilibrium phase transition governing the yielding of a soft glass*, Phys. Rev. E **89**, 062308 (2014).
- [26] S. Slotterback, M. Mailman, K. Ronaszegi, M. van Hecke, M. Girvan, and W. Losert, *Onset of irreversibility in cyclic shear of granular packings*, Physical Review E **85**, 021309 (2012).
- [27] S. Okuma, Y. Tsugawa, and a. Motohashi, *Transition from reversible to irreversible flow: Absorbing and depinning transitions in a sheared-vortex system*, Physical Review B **83**, 012503 (2011).